ACS Sustainable Chemistry & Engineering

Research Article

pubs.acs.org/journal/ascecg

Sustainable Delivery Systems: Retention of Model Volatile Oils Trapped on Hybrid Calcium Carbonate Microparticles

Amal Elabbadi,[†] Huda A. Jerri,[‡] Lahoussine Ouali,[†] and Philipp Erni*[,†]

[†]Corporate Research Division, Materials Science Department, Firmenich SA, Geneva, Switzerland

[‡]Materials Science Department, R&D North America, Firmenich, Inc., Plainsboro, New Jersey 08536, United States

Supporting Information

ABSTRACT: Transforming liquid active ingredients into solid, powdered materials is important for flavor and fragrance delivery, consumer, food, and beverage product technology, and pharmaceutical formulation. Liquid/powder blending is a sustainable technology to form liquid-loaded powders with a much lower energy input and no heating requirements as compared to heat-driven processes, such as spray-drying. The performance of wetted particles or agglomerates as delivery systems is limited because they typically remain open, without any protective barriers against loss of the liquid adsorbed on the surface and/or absorbed in the pores of the particles. Here, we investigate hybrid $CaCO_3$ microparticles precipitated in the presence of different amphiphilic additives and evaluate their capacity to trap and retain limonene, a model volatile oil, by adsorption on the particle surface. We show using a micrometer-scale analysis of localized wetting that a combination of surface area and chemical affinity of the carrier particle for the liquid is critical to control volatile losses. The specific surface area of the solid carrier particles alone is not a key parameter for good retention of volatiles in the liquid-loaded powders. Additionally, we investigate the role of highly hydrophobic, nonvolatile solvents on volatile evaporation. This study demonstrates a sustainable processing approach to form delivery systems for volatile active ingredients.

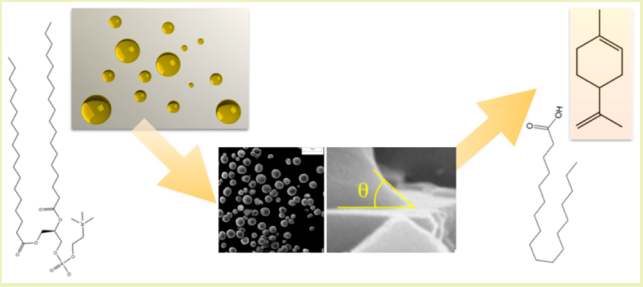

KEYWORDS: *Wetting, Capillarity, Encapsulation, Contact angle, BET, Organic/inorganic hybrid materials, Process economics*

INTRODUCTION

The transformation of liquid active ingredients into solid, powdered materials is important in many industrial areas such as flavor and fragrance delivery, consumer and cosmetic products, food technology, pharmaceutical formulation, and agrochemical deployment.[1−6] Traditionally, sensitive volatile oils including flavors and fragrances molecules or vitamins are turned into powders by processes such as spray-drying,[2,5,7] wherein emulsions of oil droplets dispersed in a concentrated polymer solution are dried in a hot gas stream to form free-flowing powders. In contrast to these thermally driven encapsulation processes, liquid/powder blending[8] is an alternative technology with a much lower energy input and no heating requirements. It is a method to transform liquid active ingredients, including flavor compounds or vitamins, into a powdered form by loading the liquid into or onto solid particles, where it is retained predominantly by surface and capillary forces. A drawback of wetted powders as delivery systems is that the particles or their agglomerates remain open, without any protective barriers against loss of the liquid adsorbed on the surface and/or absorbed in the pores of the particles.

Several materials can be considered as possible carrier particles, including organic materials such as maltodextrins or other glassy or crystalline biopolymers, inorganic particles such as porous silicon dioxide, or hybrid inorganic/organic materials. In particular, calcium carbonate ($CaCO_3$) particles are possible candidates for such applications[9−15] due to their prevalence in nature, biocompatibility, edibility as a supplement and food additive,[16,17] and tunable dissolution or chelation.

One route for calcium carbonate formation is precipitation of calcium and carbonate precursor salts. A calcium solution is contacted with a carbonate solution such that supersaturation is reached when the ionic product of the slurry is higher than the solubility product[18] of the $CaCO_3$ ($K_{sp} = 3.36 \times 10^{-9}$). In this case, $CaCO_3$ precipitation takes place spontaneously. Amorphous calcium carbonate, which is an unstable phase, first forms before being transformed into the most stable polymorph, calcite. Sawada[19] studied the mechanism of crystallization and transformation of calcium carbonate and established that the transformation of amorphous calcium carbonate into calcite proceeds by a mechanism of dissolution and recrystallization. Calcium carbonate has three different crystalline polymorphs: calcite (rhombohedral lattice and cubic shape), which is the most stable; aragonite (orthorhombic lattice and needle-like shape), which is less stable; and vaterite (hexagonal lattice and

Received: May 19, 2015
Revised: July 12, 2015
Published: July 27, 2015

DOI: 10.1021/acssuschemeng.5b00446
ACS Sustainable Chem. Eng. 2015, 3, 2178−2186

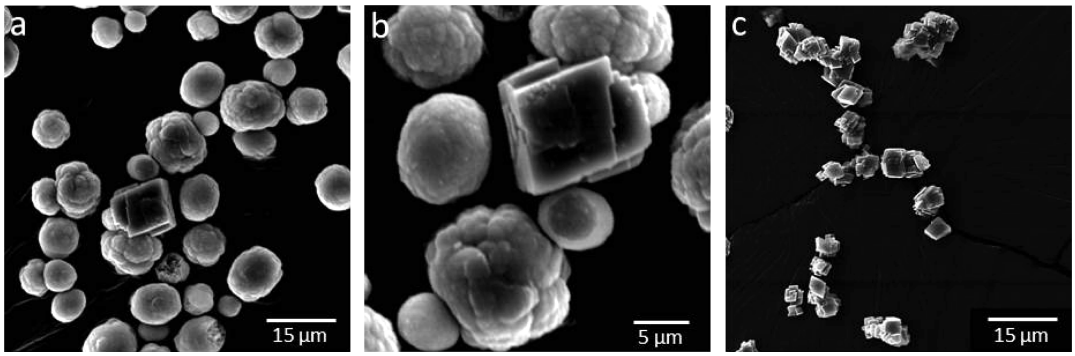

Figure 1. SEM micrographs of neat $CaCO_3$ prepared by precipitation of (a,b) 0.33 M precursor salt solutions and (c) 1 M precursor salt solutions.

generally spherical shape), which is the most unstable. Whatever the $CaCO_3$ polymorph initially formed, aging of the particles in their native slurry typically leads to their transformation into calcite, which is the most thermodynamically stable polymorph. Hence, an understanding of the process and timely quenching of the reactions are critical in order to study the effect of crystalline phase and resulting surface area and surface structures on the oil adsorption capacity.

$CaCO_3$ crystallization is thought to occur in two stages of nucleation and growth.[19] During *nucleation* the solutes start to associate into nanometer-scale clusters to form nuclei until a critical size is reached. If they are unstable, the nuclei do not reach the critical size and redissolve instead. It is during the nucleation stage that the atoms arrange to set up the crystallographic structure of the forming crystal. *Crystal growth* corresponds to the subsequent growth of the stable nuclei by uptake of the solutes in the solvent. Growth proceeds as long as the supersaturation exists. Depending on the operating conditions, either nucleation or growth can be predominant, and therefore, different crystal shapes and sizes can be obtained. As the crystal lattice and therefore the crystalline structure is determined during the nucleation stage, any "foreign" compound added during nucleation can be included in the structure and therefore modify the crystalline phase. In particular, as the (001) planes of the primary amorphous $CaCO_3$ nuclei are positively charged,[20] any negatively charged compound added during the early stages of the crystallization is likely to interact with the nuclei and therefore be included in the crystal structure. Cationic dyes and nanoparticles, such as Rhodamine 6G and amine-functionalized fluorescent polystyrene latex nanoparticles, can also be passively entrapped by adding the tracers directly into the $CaCl_2$ solution before the aggregation process is initiated through the addition of Na_2CO_3.[21−24] Incorporation of the fluorescent tracers into the composite structure has previously been confirmed with confocal microscopy.[21]

Wei et al.[25] described the effect of the nature and the concentration of sulfated (sodium dodecyl sulfate, SDS) and sulfonated (dodecylsulfonate DDS and sodium dodecylbenzenesulfonate SDBS) anionic surfactants on the crystalline phase of the resulting calcium carbonate particles. Their hybrid powders were prepared by rapidly mixing the calcium and carbonate salts in the presence of the selected surfactants. They found that vaterite crystals and hollow spherical calcite crystals could be obtained by varying the concentration of the appropriate surfactant. At SDS concentrations higher than the critical micelle concentration, micelles function as a template for the nucleation of calcite crystals. In the case of SDBS, nonhollow spherical vaterite particles are formed. The authors assume that the crystal phase is mediated by the distance between the surfactant's head groups at the surface of the micelles, which has an influence on the crystal lattice of the nuclei formed. Wan et al.[26] used lecithin liposomes as templates for the nucleation and growth of $CaCO_3$ particles to form vaterite balls and describe a strong interaction between the phosphatidyl head groups of the lecithin and the calcium cations, increasing the calcium concentration locally near the liposome surface and therefore directing the nucleation of $CaCO_3$ there before the hybrid liposome−$CaCO_3$ nanoparticles aggregated to form the so-called vaterite balls, thus reducing their surface energy.

Although significant literature is separately available on the synthesis of hybrid organic/metal salt particles and on encapsulation of volatile compounds, modification of carbonate precipitation using amphiphilic additives and the possible connection between the resulting particle shape, size, surface chemistry, and powder properties for the retention of volatile liquids trapped on the particles has not yet been explored. Here, we investigate the formation and behavior of hybrid $CaCO_3$ particles precipitated in the presence of different amphiphilic additives, and we evaluate their capacity to trap and retain volatile organic liquids using limonene as a model volatile oil. Hybrid $CaCO_3$ particles are prepared by co-precipitating the precursor calcium and carbonate ion solutions in the presence of low and high molecular weight amphiphilics such as lecithin, sodium stearate, and *Acacia* gum, a protein/polysaccharide polyampholyte.[27]

RESULTS AND DISCUSSION

Neat calcium carbonate microparticles and hybrid inorganic/organic $CaCO_3$ particles were formed using three different amphiphilic crystallization modifiers added during the precipitation step: (1) *Lecithin* is a naturally occurring emulsifier composed of fatty acid hydrophobic chains and a zwitterionic headgroup comprising a phosphate group (negatively charged) and a quaternary amine (positively charged). Phosphate groups can interact with calcium ions, promoting incorporation of the phospholipid into the $CaCO_3$ structure. Furthermore, the fatty acid chain is expected to increase the affinity of the particles for the oil phase. (2) *Sodium stearate*, fatty acid monolayers, have previously been used to precipitate interfacial films of crystalline and amorphous calcium carbonate.[11,28] They are the most hydrophobic of the additives studied here, and it can be expected that fatty acids present on metal salt particles strongly influence the wetting properties due to the presence of long hydrocarbon chains. (3) *Acacia gum*, also known as Gum

DOI: 10.1021/acssuschemeng.5b00446
ACS Sustainable Chem. Eng. 2015, 3, 2178−2186

Arabic, is a macromolecular amphiphile containing both protein and polysaccharide subunits and is negatively charged at the pH values of interest in the aqueous phase.[27]

Scanning electron microscopy was used to characterize the morphology of the particles. The particle morphology strongly depends on the initial precursor salts' concentrations, with higher ionic strengths leading to a greater incidence of calcite microstructures. As shown in Figure 1a and b, particles precipitated from 0.33 M precursor salts solutions are primarily present as nearly spherical calcium carbonate microspheres, although a minor population of calcite rhombohedra was also observed. FTIR spectra (Figure 2) in combination with the SEM micrographs suggest that the microparticles are vaterite polymorphs, as indicated by a small but highly characteristic double peak[29] in the transmission spectra at a wavenumber around 1080 cm^{-1}; reference calcite and vaterite were prepared as described previously.[21,23,24] In contrast, higher concentrations with equal volumes of 1 M in the precursor salt solutions lead to exclusive formation of layered rhombohedral calcite crystals (Figure 1c).

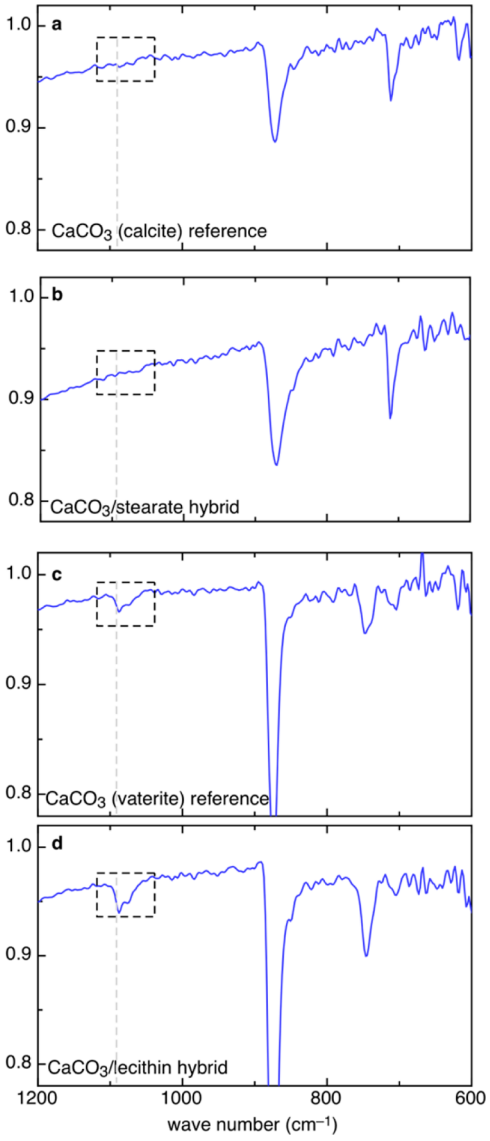

Figure 2. FTIR spectra of reference calcite and the $CaCO_3$–stearate hybrid particles (a,b) and of the spherical vaterite and $CaCO_3$–lecithin hybrid particles (c,d). Dashed boxes indicate the region of the characteristic double peaks in the case of vaterite polymorphs[29] around a wavenumber of 1080 cm^{-1} (gray dashed lines).

The particle morphology and size is further influenced by the type of amphiphilic crystallization modifiers used during the reaction. While small, near-spherical microparticles were formed using lecithin (Figure 3a), mostly rhombohedral

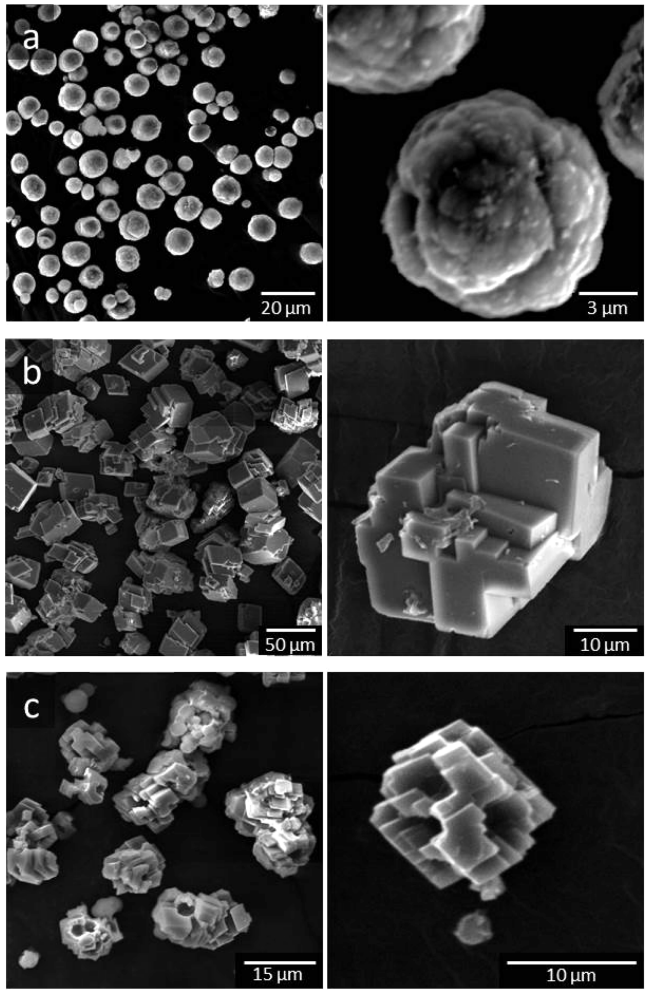

Figure 3. SEM micrographs of the hybrid $CaCO_3$ microparticles co-precipitated with (a) lecithin ($CaCO_3$ concentration during precipitation, 0.27 M; lecithin concentration, 3.86 g/L), (b) sodium stearate (0.33 M $CaCO_3$; 0.183 mM sodium stearate) and (c) *Acacia* gum (0.33 M $CaCO_3$; 4.55 g/L Acacia gum).

particles were observed for the other two modifiers (sodium stearate in Figure 3b and *Acacia* gum in Figure 3c). Particles formed with sodium stearate were significantly larger (Figure 3b), and by comparison with reference samples, their FTIR spectra suggest that the particles are calcite polymorphs.

The specific surface areas of the particles were determined by nitrogen sorption and BET (Brunauer–Emmett–Teller) analysis of the sorption isotherms. As detailed in Table 1, the greatest specific surface area was found for the neat $CaCO_3$ microparticles. Chemical modification of the precipitated $CaCO_3$ decreased the specific area in all cases. The BET results are confirmed by the morphology analysis based on the SEM micrographs; $CaCO_3$–stearate forms dense particles with its smooth, rhombohedral layers and low specific surface area. $CaCO_3$–AG particles have a slightly increased surface rough-

DOI: 10.1021/acssuschemeng.5b00446
ACS Sustainable Chem. Eng. 2015, 3, 2178–2186

Table 1. Moisture and Organic Contents and Specific Surface Area S_{spec} Measured by Nitrogen Sorption Isotherms and BET Analysis for the Neat and Hybrid $CaCO_3$ Powders

	$CaCO_3$	$CaCO_3$–AG	$CaCO_3$–lecithin	$CaCO_3$–stearate
moisture content (%)	2.2	1.6	2.0	0
organic content (%)	0.0	7.6	4.0	1.5
S_{spec} (m^2/g)	30	8.9	22.9	7.7

ness and a slightly higher specific surface area. Finally, the $CaCO_3$–lecithin particles are nearly spherical and display fissures on their surfaces similar to the neat $CaCO_3$ particles, but with a slightly smaller mean particle size, a more uniform shape, and a smoother surface morphology. The specific surface area of this hybrid material is higher than for the two other additives but still lower than that of the neat precipitated $CaCO_3$ microspheres. With the relatively low specific surface areas observed here, we assume that the particles differ primarily in their surface structure, as shown in SEM micrographs, whereas intraparticle porosity is negligible.

In addition to the specific surface area measurements, thermogravimetric (TGA) experiments were performed to obtain the organic content in the hybrid particles. Two different steps can be distinguished in the TGA analyses (Supporting Information) corresponding to the moisture evaporation at times up to 10 min (approximately $T < 230$ °C) and the degradation of the organic material after 10 min (approximately $T > 230$ °C). Neat $CaCO_3$ is the reference sample (purely inorganic), therefore, its weight loss during the analysis only corresponds to its moisture content, which is 2.2% w/w. The $CaCO_3$–stearate hybrid powder does not contain significant moisture, and its weight loss is therefore only due to the degradation of the organic part, resulting in an organic content of 1.5% w/w in the particles. The $CaCO_3$–AG hybrid powder contains 1.6% w/w of moisture and 7.6% w/w of organic matter, and the $CaCO_3$–lecithin powder contains 2% w/w of moisture and 4% w/w organic matter. These results are summarized in Table 1.

Figure 4 shows number-based particle size distributions for the different hybrid particles, as extracted from the SEM images using image analysis. Both the normalized number fractions, and the cumulative distribution functions are shown. The Feret diameter (longest secant diameter of the projected particle) is used as the characteristic particle size. The distributions of the neat $CaCO_3$ microspheres and the $CaCO_3$–lecithin hybrid

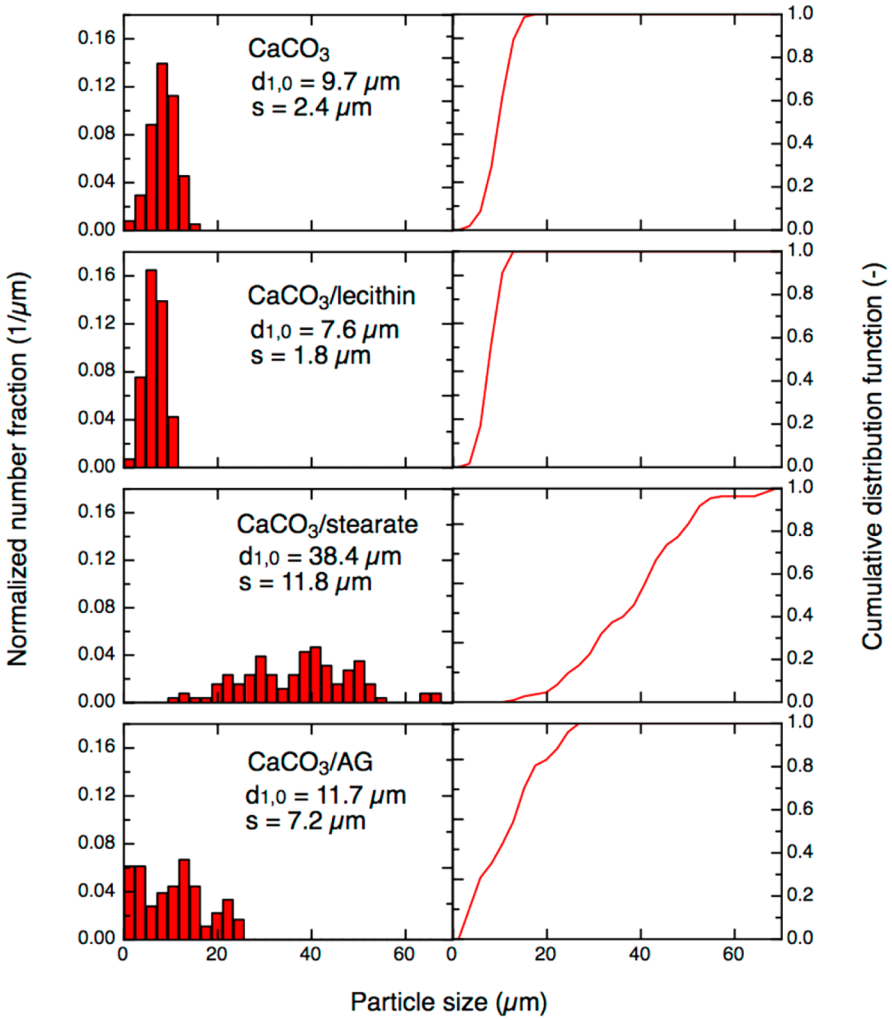

Figure 4. Particle size distributions of the different hybrid particles. Left: normalized number fractions. Right: Cumulative distribution function. The Feret diameter (longest secant diameter) is used as the particle size ($d_{1,0}$, number-based mean diameter from SEM image analysis; s, standard deviation).

DOI: 10.1021/acssuschemeng.5b00446
ACS Sustainable Chem. Eng. 2015, 3, 2178–2186

particles are very similar. Microparticles formed in the presence of lecithin are slightly smaller ($d_{1,0}$ = 7.6 ± 1.8 μm) than the neat $CaCO_3$ ($d_{1,0}$ = 9.7 ± 2.4 μm), and their size distribution is the most uniform (least polydisperse) of all samples. The $CaCO_3$–stearate particles are the largest and the most polydisperse ($d_{1,0}$ = 38.4 ± 11.8 μm), followed by the $CaCO_3$–AG ($d_{1,0}$ = 11.8 ± 7.2 μm) hybrid particles.

In Figure 5, different particle shape parameters are plotted, as obtained from image analysis of the projected images in SEM micrographs for the different hybrid particle populations. All shape parameters are summarized in the form of box plots. Shown are the *circularity* $4\pi(A/p^2)$, the *aspect ratio* of the longest and shortest secant diameter of a projected particle, and *convex hull solidity* A/A_{cv}, describing the degree of particle

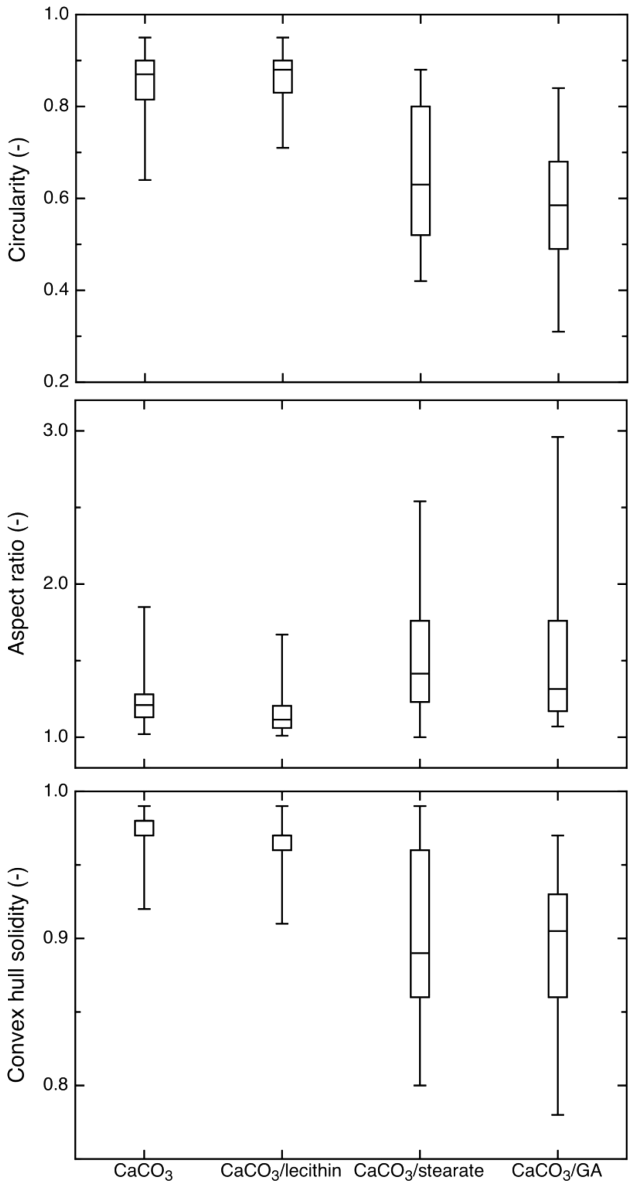

Figure 5. Summary of the shape parameters obtained from projection analysis in SEM micrographs for the different hybrid particle populations, represented as box plots. The plots show the circularity $4\pi(A/p^2)$, the aspect ratio of the longest and shortest secant diameter of a projected particle, and convex hull solidity A/A_{cv}, where A is the projected area, p is the perimeter of an individual particle, and A_{cv} is the area of the projected particle's convex hull.

"compactness", where A is the projected area, p is the perimeter of an individual particle, and A_{cv} is the area of the projected particle's convex hull. This shape analysis provides a quantitative summary and facilitates direct comparison between the morphologies of these particle populations. Neat $CaCO_3$ and $CaCO_3$–lecithin particles have similar distributions of all shape parameters; both are compact particles with an almost sphere-like shape with similar median values. The distributions of all shape parameters are the narrowest for the $CaCO_3$–lecithin system. $CaCO_3$–stearate and $CaCO_3$–*Acacia* gum particles are nonspherical and exhibit jagged surface structures.

Among the four types of particles evaluated here, two are formed in the presence of amphiphilic additives containing strongly hydrophobic portions, i.e., the fatty acid side chains in the lecithin and the sodium stearate, whereas the other two are expected to be more hydrophilic in nature (neat calcium carbonate and the hybrid particles with *Acacia* gum, which does contain hydrophobic regions but overall is a water-soluble proteoglycan). To investigate the surface chemistry and clarify the role of wetting phenomena on particles with presumed differences in surface affinity toward oils, we performed model wetting experiments using PDMS/particle/gas contact lines. Instead of using small molecular weight volatile oils, we wetted the particles with higher molecular weight silicone oil and subsequently polymerized this oil to form solid PDMS, thereby "freezing" the three-phase contact line for electron microscopy imaging. Figure 6 displays typical SEM micrographs showing

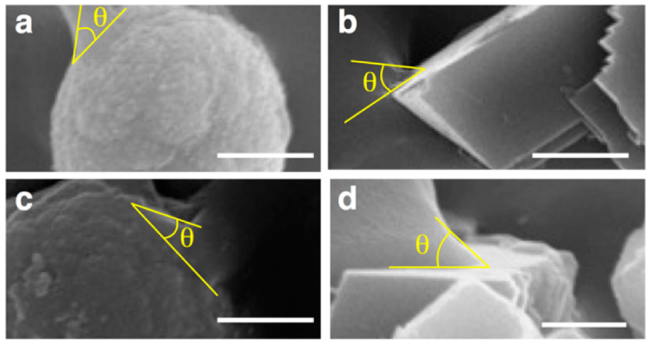

Figure 6. SEM micrographs showing the local contact line of PDMS wetting the hybrid particles. The liquid PDMS was made to wet the particles, and was then polymerized, solidified, and sliced for imaging. The panels show neat $CaCO_3$ particles (a), $CaCO_3$–stearate hybrids (b), $CaCO_3$–lecithin hybrids (c), and $CaCO_3$–*Acacia* gum hybrids (d).

the local contact line of polymerized PDMS bridges wetting the hybrid particles at the length scale of a few micrometers. Multiple SEM images were screened for such contact locations oriented roughly perpendicularly to the plane of imaging, and the contact angles were measured using image analysis software. The mean values of the projected contact angles are in the range of 78–88° for all samples, and the values are strongly scattered with standard deviations around ±25°. These local variations in the wetting behavior suggest a strong wetting heterogeneity on the particle surfaces at the micrometer length scale, even for the neat $CaCO_3$ particles. Differences in surface roughness between the particles observed in the SEM micrographs on the length scales of 0.1–100 μm do not appear to influence this inhomogeneity in wetting properties. We calculated several statistical measures for these contact angle distributions for each particle population, including mean

DOI: 10.1021/acssuschemeng.5b00446
ACS Sustainable Chem. Eng. 2015, 3, 2178–2186

and quantile values, kurtosis, skewness, and polydispersity of the contact angles. Along with the particle morphology data, we will use those parameters to assess the different particle types in comparison with their ability to retain volatile oils trapped in the liquid/particle blends.

To track the liquid content in the oil-loaded particles, we performed repeated thermogravimetry experiments over the course of several weeks, drawing samples of the loaded powders at defined time intervals. The evolution of the normalized oil content in the plated samples over time is shown in Figure 7 for powders containing an initial volatile oil mass fraction at time t = 0 of 20% w/w (corresponding to the normalized value of 1 at t = 0).

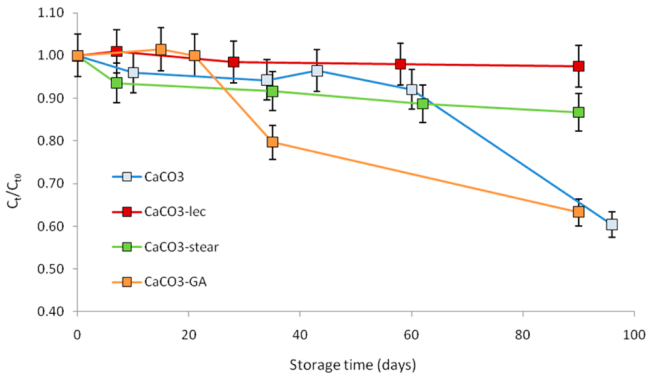

Figure 7. Evolution of the volatile oil content in the liquid-loaded microparticle powders with time. Volatile mass fraction at time t = 0:20% w/w. C_t/C_{t0} is the volatile mass fraction C_t at time t normalized with the mass fraction at time 0.

Next, the effect of amphiphilic crystallization modifiers on the retention of volatile oils loaded on the powders is assessed by thermogravimetric analysis. The chemical modification of the calcium carbonate particles to tune the hydrophobicity and specific surface area of the carriers was expected to have two possible effects on oil uptake and retention. The first hypothesis was that the higher the specific surface area of the powder would lead to greater oil absorption capacity,[30] and the second hypothesis was that the more hydrophobic particles would also have greater absorption and retention of plated oils. In particular, modification of the particles with lecithin and stearic acid (containing fatty acid chains) is likely to increase the surface hydrophobicity of the particles[31] and therefore their affinity with oil. After preparing the free-flowing samples as described in the Experimental Section (all the samples were prepared with 20% w/w limonene and 80% w/w solid carrier particles), they were stored in capped glass vials in the lab, and TGA measurements were run regularly over time to determine the amount of volatile remaining in the powders.

The normalized graphs were obtained by determining the volatile oil content using TGA at the different storage times. At the end of the analyses when all the flavor has evaporated, the plateau gives an indication of the flavor content. Then, the volatile oil content at time t was divided by the initial oil content at time t_0. Thus, the normalized graphs in Figure 7 display the evolution of the relative oil content over time.

According to Figure 7, the particles modified with lecithin and stearate retained the most limonene. In particular, $CaCO_3$–lecithin shows minimal loss after 3 months of storage at room temperature. In contrast, pure $CaCO_3$ and $CaCO_3$–AG do not retain the volatile oil as well, with 40% loss after 3 months. Moreover, the hybrid $CaCO_3$–AG carrier retains the limonene even less than pure $CaCO_3$, as sudden loss appears after 21 days for $CaCO_3$–AG, compared to 60 days for pure $CaCO_3$.

With the size, shape, and contact angle distributions and measurements available, we are able to assess the retention capacity of the powders with respect to the physicochemical properties of the particles using the remaining normalized volatile load after 90 days of storage as a measure of the retention capacity. The following parameters were evaluated against this retention capacity: mean particle size, median particle size and several quantiles of the particle size distribution, maximum and minum particle size polydispersity of size, shape, projected circularity, particle aspect ratio, and convex hull solidity. Interestingly, none of these quantities demonstrated significant correlation with the oil retention capacity. Anecdotally, large $CaCO_3$–stearate particles retain the oil very well, but so do the much smaller $CaCO_3$–lecithin particles. Likewise, the particles with the highest specific surface area are not necessarily the most suitable carrier for liquid loading. For instance, $CaCO_3$–stearate has the smallest specific surface area but is nevertheless more efficient than the neat $CaCO_3$ in retaining the volatile oil. Finally, none of the powder

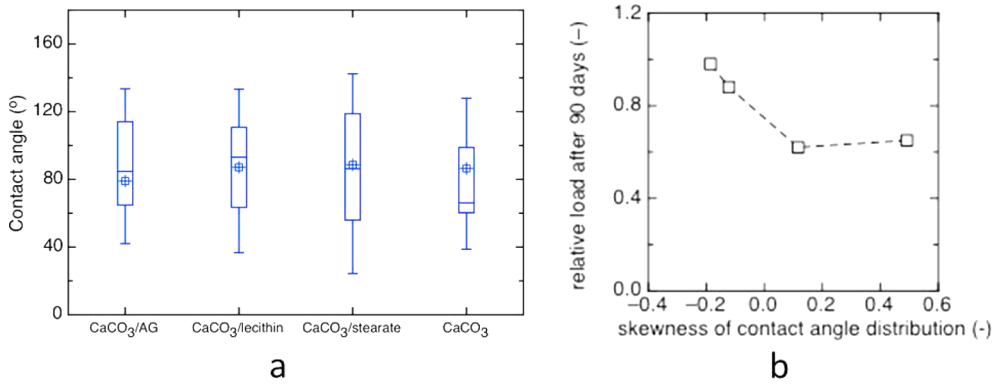

Figure 8. Analysis of the microscopic contact angle measurements. (a) Box plots showing the median, upper, and lower quartile values (boxes), mean values (squares), and the far outliers (end lines). The mean values for each particle population are similar (θ_{CaCO3} = 79° ± 22°, $\theta_{CaCO3,lecithin}$ = 89° ± 23°, $\theta_{CaCO3,stearate}$ = 87° ± 32°, $\theta_{CaCO3,AG}$ = 86° ± 24°) and are not correlated to the retention of volatile oil in the powders. (b) Relative volatility as a function of the skewness of the contact angle distribution. The more skewed the distribution is toward small contact angles, the better the volatile retention is.

DOI: 10.1021/acssuschemeng.5b00446
ACS Sustainable Chem. Eng. 2015, 3, 2178−2186

characteristics (porosity and bulk powder density) of the particles before liquid loading were significantly correlated with the final oil load. In contrast, Figure 7 shows that the hybrid $CaCO_3$ particles containing either lecithin or sodium stearate, i.e., those containing the more hydrophobic amphiphiles with fatty acid side chains, have much better oil retention capacity, in contrast to the more hydrophilic *Acacia* gum-modified and neat $CaCO_3$. Hence, the greatest stability of the plated powders depends on the choice of the suitable carrier for a given volatile oil. The more affinity the volatile has for the carrier, the less likely it is to evaporate.

Assuming that higher affinity of the oil for the particles is reflected by a smaller contact angle of the oil/particle/gas interface, we investigated the role of the contact angle of the different particles. As shown in Figure 8, the wetting properties of the particles are highly heterogeneous, resulting in large standard deviations and similar mean values of the microscopic contact angles obtained with a hardened nonvolatile oil as a model system. The mean and median contact angles are therefore poor predictors for oil retention. A close look at Figure 8, however, reveals that for the lecithin- and stearate-modified particles, the distribution of contact angles trends toward smaller values. This characteristic can be quantified using the *skewness* parameter of the distribution $sk = (1/n)\sum_1^n(((\theta_i - \bar{\theta})/\sigma)^3)$ (calculated as Pearson's third standardized moment of the distribution[32]), and indeed, we find that for the more hydrophobic additives the skewness of the distribution of local contact angles is a suitable predictor for the particles' ability to trap volatiles. Given the relatively small fraction of the amphiphilic additives in the particles, we propose that the additives may create heterogeneous hydrophobic "patches" on the particles, rather than a uniform coating, and those patches are key to enhanced wetting of the oil, resulting in improved stability against oil evaporation.

In addition to the surface chemistry and structure of the particles, another approach to increase the affinity of the volatile for the liquid-loaded powder is to add a nonvolatile, highly hydrophobic solvent to the volatile oil (Figure 9). In the case of limonene, which has a logarithmic octanol/water partition coefficient (logP value) of 4, we have added a nonvolatile, highly hydrophobic oil (MCT; caprilic/capric acid ester medium-chain triglyceride). Three samples were made by preparing mixtures of different limonene/MCT ratios and loaded onto the carrier powder.

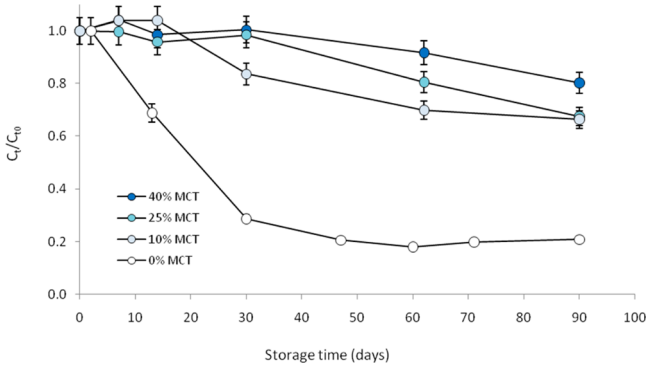

Figure 9. Effect of the addition of highly hydrophobic, nonvolatile components on volatile retention. Medium chain triglyceride (MCT, given in % w/w) oil was used as a nonvolatile, highly hydrophobic additive to the volatile oil. The curves show the evolution of the limonene content as a function of the MCT/limonene weight ratio. C_t/C_{t0} is the normalized volatile mass fraction over time.

As shown in Figure 9, the presence of the nonvolatile, highly hydrophobic solvent strongly influences the loss of the more volatile component. As more MCT oil was added in the liquid mixture, the loss of volatile oil over time was reduced and the more volatile oil remained trapped in the wetted powder. The rate of evaporation is proportional to the difference in chemical potential between the liquid and gas phases.[33,34] Here, this effect is influenced via the liquid phase composition by the addition of MCT; the lower the limonene volume fraction is in the liquid mixture with the highly hydrophobic solvent, the lower is its evaporation rate.

CONCLUSIONS

We demonstrate the improvement in volatile retention properties of an inorganic carrier, calcium carbonate, through generation of composite carriers and modification of the gas/liquid partitioning using highly hydrophobic, low volatility (co)solvents. We have shown that chemical modification of the particles by co-precipitation with hydrophobic surfactants such as lecithin or sodium stearate results in particles with different physical characteristics including morphology, crystalline phase, specific surface area, and moisture content. Composite carrier particles have a higher affinity for volatile flavor and fragrance molecules, such as limonene, which makes them ideal candidates for liquid/powder blending. As evidenced through the monitoring of volatile loss over time, plated samples prepared with lecithin or sodium stearate-modified $CaCO_3$ retained about 50% more limonene after 3 months of storage as compared to pure calcium carbonate. On the contrary, *Acacia* gum-modified $CaCO_3$ did not have any retention effect with limonene, as compared to pure $CaCO_3$. We attribute this performance to the interaction between fatty acid chains and the volatile molecules. This effect can also be mimicked without chemical modification by adding a nonvolatile hydrophobic solvent to the volatile oil prior to plating. We have shown that the physicochemical affinity between the carrier and the volatile payload oil is essential for volatile retention, while high specific surface area alone is not a key criterion to formulate and process stable liquid-loaded powders. We point out that our approach discussed here focuses primarily on the issues of physical stabillity and loss reduction of precipitated particles as delivery systems for volatile molecules. In contrast to spray-dried or extruded microcapsules,[35] the liquid-loaded particles studied here remain open and do not provide a diffusion barrier. Therefore, if the liquid phase contains compounds that are very sensitive to degradation, the issue of chemical degradation still needs to be addressed separately, e.g., by chemical stabilization via the liquid phase formulation[36,37] or additional coatings.[38]

EXPERIMENTAL SECTION

Materials. Calcium chloride anhydrous powder was purchased from Acros Organics. Sodium carbonate was purchased from VWR Prolabo. Lecithin was purchased from Acros Organics. *Acacia* gum (Gum Arabic) was supplied by Nexira. Stearic acid, sodium salt 96%, was purchased from Acros Organics. Neobee M5 (medium chain triglyceride) was supplied by Stepan. All products were used as received. All other chemicals were obtained from Sigma-Aldrich. Limonene (1-methyl-4-(1-methylethenyl)-cyclohexene) was used as a model volatile active compound.

Precipitation of the $CaCO_3$-Based Microparticles. *$CaCO_3$.* Equal volumes of 0.33 M Na_2CO_3 and $CaCl_2$ solution were prepared

DOI: 10.1021/acssuschemeng.5b00446
ACS Sustainable Chem. Eng. 2015, 3, 2178−2186

(8.75 g of Na_2CO_3 was dissolved in 250 mL of deionized water, and 9.54 g of $CaCl_2$ 96% wase dissolved in 250 mL of deionized water using graduated flasks). Then, the Na_2CO_3 solution was added to the $CaCl_2$ solution under stirring, and a milky suspension of $CaCO_3$ particles immediately formed as described in the literature.[21−24] After 20 min, 250 mL of deionized water was added to the slurry to quench the reaction, and the suspension was allowed to sediment. The supernatant was again removed, and the precipitate was rinsed with DI water, repeating the sedimentation and resuspension steps to remove excess salts and prevent further reaction. The rinsed and concentrated $CaCO_3$ solids were then dried at room temperature in a dish.

$CaCO_3$−Lecithin Hybrid Particles. One g of lecithin (corresponding to 1.3 mmol) was dissolved in a hydro-alcoholic mixture containing 49 g of DI water and 10 g of ethanol, while heating at 40 °C. 100 mL of 0.27 M $CaCl_2$ solution was added slowly under stirring. The mixture was stirred for 30 min to promote the interaction between the Ca^{2+} ions and the lecithin head groups, and we could observe the formation of small particles. Then, 100 mL of a 0.27 M Na_2CO_3 solution was added while stirring to complete the hybrid particle formation. A total of 100 mL of DI water was finally added to quench the reaction by dilution, before removing the supernatant, rinsing the solid phase with DI water and drying it at room temperature in a polyacrylic Petri dish.

$CaCO_3$−Stearate Hybrid Particles. A total of 43 mg of Na-stearate (0.1 mmol, ACROS) was dissolved in 46 g of warm water while heating at 40 °C for 1 h. Meanwhile, 250 mL of 0.33 M $CaCl_2$ and 0.33 M Na_2CO_3 solutions was prepared in DI water. Then, the Na-stearate solution was slowly added to the calcium chloride solution under stirring. After a few milliliters were added, a precipitate formed. The rest of the Na-stearate solution was added to the carbonate solution under stirring, where a precipitate formed as well. To complete the $CaCO_3$−stearate hybrid particle formation, the carbonate solution was added to the calcium solution under strong stirring, and the slurry was stirred for 15 min at room temperature before being allowed to sediment. The supernatant was removed carefully, and the solid phase was rinsed twice with DI water before being dried at room temperature.

$CaCO_3$−Acacia Gum Hybrid Particles. One gram of *Acacia* gum, Eficacia (Nexira, France), was dissolved in 110 mL of 0.33 M $CaCl_2$. Then, 110 mL of 0.33 M Na_2CO_3 solution was added to the previous mixture under stirring. The slurry was stirred for 15 min before quenching the reaction with 100 mL of DI water and removing the supernatant. The solid phase was rinsed twice with DI water and was then dried at room temperature in a polyacrylic dish.

Specific Surface Area Measurements. The specific surface area of the hybrid microparticles was measured by the nitrogen sorption method using a Nova 1000 Series surface area analyzer (Quantachrome). The powders were degassed in a desiccator containing anhydrous sodium sulfate under vacuum and at room temperature for 2 weeks and for an additional 3 h in the instrument at 80 °C prior to the measurements. After degassing, a weighed amount of the clean powder was transferred into the measurement cell and cooled to −195.75 °C (77.4 K) by immersion in liquid nitrogen. Starting from vacuum, small amounts of nitrogen gas were introduced by increasing p/p_0 in steps, allowing the N_2 sorption onto the particle surface. The BET theory was used to calculate the monolayer-covered surface as $(1/(v[p_0/p - 1])) = ((c - 1)/(v_m c))\ (p/p_0) + (1/(v_m c))$ (v, volume of adsorbed gas; p_0, saturation pressure of the adsorbate at the temperature of adsorption; p, equilibrium pressure of the adsorbate at the temperature of adsorption; v_m, volume of the monolayer adsorbed gas; and $c = \exp[(E_1 - E_L)/RT]$ is the BET constant, where E_1 is the heat of adsorption of the first layer of adsorbate, E_L is the heat of adsorption of the second and higher layer, R is the universal gas constant, and T is temperature).

Scanning Electron Microscopy (SEM). SEM imaging was performed using JEOL JSM-T330 and JSM-6010LA scanning electron microscopes. An accelerating voltage of 15.0 kV was used for all samples. The microparticles were pressed onto carbon tape, which was pre-adhered to an aluminum stub. Excess powder was tapped off. The mounted samples were then sputter-coated with cold gold/palladium plasma for 1 min to reduce charging effects during imaging.

Fourier Transform Infrared Spectroscopy (FTIR). FTIR was performed on the precipitated microparticles using a Vertex 70 spectrometer (Bruker, Switzerland) with a room temperature DLaTGS type detector and a mid-infrared light source in attenuated total reflection mode (Specac Golden Gate ATR accessory).

Preparation of Liquid-Loaded Powders Using the Hybrid Microparticles. The liquid/powder blends were prepared using a laboratory scale powder blender; small quantities were prepared by simply dosing the required amount of liquid onto the powder with a pipet and using a mortar and pestle and blending for 30 s to obtain a homogeneous powder. The samples obtained were transferred into screw-capped glass vials for storage.

Thermogravimetric Analysis. (i) Determination of the organic content in the hybrid particles: To determine the amount of lecithin, sodium stearate, or *Acacia* gum in the hybrid $CaCO_3$, the powders were calcined using a thermogravimetric analyzer (TGA/SDTA 851e from Mettler Toledo) using the following temperature program: (1) heating from 30 to 500 °C at a rate of 20 °C/min and (2) maintaining the temperature at 500 °C for 10 min. *(ii) Time-dependent measurements of oil content in the volatile-loaded powders:* TGA measurements were also performed to monitor the volatile oil content of the liquid-loaded powders over time. A few milligrams of the sample were transferred into a pre-weighed aluminum crucible, which was then heated using the following program: (1) heating from 30 to 120 °C, following a linear temperature ramp of 20 °C/min and (2) maintaining the sample's temperature at 120 °C for 10 min. This analysis provides information about the amount of liquid (volatile oil + possible moisture) retained in the sample over time and therefore provides information about the suitability of the powders as oil carriers and delivery systems.

■ ASSOCIATED CONTENT

Ⓢ Supporting Information

Additional thermogravimetry data. The Supporting Information is available free of charge on the ACS Publications website at DOI: 10.1021/acssuschemeng.5b00446.

■ AUTHOR INFORMATION

Corresponding Author

*E-mail: philipp.erni@firmenich.com.

Notes

The authors declare no competing financial interest.

■ REFERENCES

(1) Day, L.; Seymour, R. B.; Pitts, K. F.; Konczak, I.; Lundin, L. Incorporation of functional ingredients into foods. *Trends Food Sci. Technol.* **2009**, *20*, 388−395.

(2) Serfert, Y.; Schröder, J.; Mescher, A.; Laackmann, J.; Shaikh, M. Q.; Rätzke, K.; Gaukel, V.; Schuchmann, H. P.; Walzel, P.; Moritz, H.-U.; Drusch, S.; Schwarz, K. Characterization of the spray drying behavior of emulsions containing oil droplets with a structured interface. *J. Microencapsulation* **2013**, *30*, 325−334.

(3) Deng, J.; Yang, B.; Chen, C.; Liang, J. Renewable Eugenol-Based Polymeric Oil-Absorbent Microspheres: Preparation and Oil Absorption Ability. *ACS Sustainable Chem. Eng.* **2015**, *3*, 599−605.

(4) Erni, P.; Dardelle, G.; Sillick, M.; Wong, K.; Beaussoubre, P.; Fieber, W. Turning Coacervates into Biohybrid Glass: Core/Shell Capsules Formed by Silica Precipitation in Protein/Polysaccharide Scaffolds. *Angew. Chem., Int. Ed.* **2013**, *52*, 10334−10338.

(5) Madene, A.; Jacquot, M.; Scher, J.; Desobry, S. Flavour encapsulation and controlled release - A review. *Int. J. Food Sci. Technol.* **2006**, *41*, 1−21.

(6) Pretzl, M.; Neubauer, M.; Tekaat, M.; Kunert, C.; Kuttner, C.; Leon, G.; Berthier, D.; Erni, P.; Ouali, L.; Fery, A. Formation and Mechanical Characterization of Aminoplast Core/Shell Microcapsules. *ACS Appl. Mater. Interfaces* **2012**, *4*, 2940.

DOI: 10.1021/acssuschemeng.5b00446
ACS Sustainable Chem. Eng. 2015, 3, 2178−2186

(7) Normand, V.; Subramaniam, A.; Donnelly, J.; Bouquerand, P. E. Spray Drying: Thermodynamics and Operating Conditions. *Carbohydr. Polym.* **2013**, *97*, 489.
(8) Bolton, T. A.; Reineccius, G. A. The oxidative stability and retention of a limonene-based model flavor plated on amorphous silica and other selected carriers. *Perfum. Flavor.* **1991**, *17*, 1−22.
(9) Page, M. G.; Nassif, N.; Börner, H. G.; Antonietti, M.; Cölfen, H. Mesoporous Calcite by Polymer Templating. *Cryst. Growth Des.* **2008**, *8*, 1792−1794.
(10) Gehrke, N.; Cölfen, H.; Pinna, N.; Antonietti, M.; Nassif, N. Superstructures of Calcium Carbonate Crystals by Oriented Attachment. *Cryst. Growth Des.* **2005**, *5*, 1317−1319.
(11) Maas, M.; Rehage, H.; Nebel, H.; Epple, M. On the formation of calcium carbonate thin films under Langmuir monolayers of stearic acid. *Colloid Polym. Sci.* **2007**, *285*, 1301−1311.
(12) Maas, M.; Rehage, H.; Nebel, H.; Epple, M. A detailed study of closed calcium carbonate films at the liquid/liquid interface. *Langmuir* **2009**, *25*, 2258−2263.
(13) DiMasi, E.; Patel, V. M.; Sivakumar, M.; Olszta, M. J.; Yang, Y. P.; Gower, L. B. Polymer-Controlled Growth Rate of an Amorphous Mineral Film Nucleated at a Fatty Acid Monolayer. *Langmuir* **2002**, *18*, 8902−8909.
(14) Cölfen, H. Bio-inspired Mineralization Using Hydrophilic Polymers. *Top Curr. Chem.* **2007**, *271*, 1−77.
(15) Cölfen, H. Precipitation of carbonates: recent progress in controlled production of complex shapes. *Curr. Opin. Colloid Interface Sci.* **2003**, *8*, 23−31.
(16) Direct Food Substances affirmed as generally recognized as safe, Calcium Carbonate. *Code of Federal Regulations*, Chapter I, SubChapter B, Section 184, Title 21, 21CFR184.1191, U.S. Food and Drug Administration, 2014.
(17) European Food Safety Authority (EFSA) Panel on Food Additives and Nutrient Sources added to Food. Scientific Opinion on Re-Evaluation of Calcium Carbonate (E170) as Food Additive. *EFSA Journal* **2011**, *9*, 2318.
(18) *CRC Handbook of Chemistry and Physics*, 95th ed.; Taylor and Francis, 2015.
(19) Sawada, K. The mechanism of crystallization and transformation of calcium carbonates. *Pure Appl. Chem.* **1997**, *69*, 921−928.
(20) Xu, G.; Yao, N.; Aksay, I. A.; Groves, J. T. Biomimetic Synthesis of Macroscopic-Scale Calcium Carbonate Thin Films. Evidence for a Multistep Assembly Process. *J. Am. Chem. Soc.* **1998**, *120*, 11977−11985.
(21) Jerri, H. *Fabrication of Anisotropic Multifunctional Colloidal Carriers; $CaCO_3$ Matrix Microparticles Embedded with Fluorescent Tracer Nanoparticles*. Doctoral Dissertation, Pennsylvania State University, State College, PA, 2010.
(22) Volodkin, D. V.; Larionova, N. I.; Sukhorukov, G. B. *Biomacromolecules* **2004**, *5*, 1962−1972.
(23) Erni, P.; Elabbadi, A. Free Impinging Jet Microreactors: Controlling Reactive Flows via Surface Tension and Fluid Viscoelasticity. *Langmuir* **2013**, *29*, 7812−7824.
(24) Elabbadi, A.; Jeckelmann, N.; Haefliger, O.; Ouali, L.; Erni, P. Selective Coprecipitation of Polyphenols in Bioactive/Inorganic Complexes. *ACS Appl. Mater. Interfaces* **2011**, *3*, 2764−2771.
(25) Wei, H.; Shen, Q.; Zhao, Y.; Zhou, Y.; Wang, D.; Xu, D. On the crystallization of calcium carbonate modulated by anionic surfactants. *J. Cryst. Growth* **2005**, *279*, 439−446.
(26) Wan, P.; Zhao, Y.; Tong, H.; Yang, Z.; Zhu, Z.; Shen, X.; Hu, J. The inducing effect of lecithin liposome organic template on the nucleation and crystal growth of calcium carbonate. *Mater. Sci. Eng., C* **2009**, *29*, 222−227.
(27) Erni, P.; Parker, A. Nonlinear viscoelasticity and shear localization at complex fluid interfaces. *Langmuir* **2012**, *28*, 7757−7767.
(28) DiMasi, E.; Kwak, S. Y.; Amos, F. F.; Olszta, M. J.; Lush, D.; Gower, L. B. Complementary Control by Additives of the Kinetics of Amorphous $CaCO_3$ Mineralization at an Organic Interface: In-Situ Synchrotron X-Ray Observations. *Phys. Rev. Lett.* **2006**, *97*, 045503.
(29) Sato, M.; Matsuda, S. Structure of vaterite and infrared spectra. *Z. Kristallogr.* **1969**, *129*, 405−410.
(30) Adelmann, H.; Binks, B. P.; Mezzenga, R. Oil Powders and Gels from Particle-Stabilized Emulsions. *Langmuir* **2012**, *28*, 1694−1697.
(31) Osman, M. A.; Suter, U. W. Surface Treatment of Calcite with Fatty Acids: Structure and Properties of the Organic Monolayer. *Chem. Mater.* **2002**, *14*, 4408−4415.
(32) Joanes, D. N.; Gill, C. A. Comparing measures of sample skewness and kurtosis. *J. Royal Stat. Soc.: Series D* **1998**, *47*, 183−189.
(33) Bird, R. B.; Stewart, W. E.; Lightfoot, E. N. *Transport Phenomena*, revised 2nd ed.; Wiley: New York, 2007.
(34) Parker, A.; Babas, R. Thermogravimetric measurement of evaporation: Data analysis based on the Stefan tube. *Thermochim. Acta* **2014**, *595*, 67−73.
(35) Drusch, S.; Berg, S. Extractable oil in microcapsules prepared by spray-drying: localisation, determination and impact on oxidative stability. *Food Chem.* **2008**, *109*, 17−24.
(36) Agustin-Salazar, S.; Gamez-Meza, N.; Medina-Juàrez, L. A.; Soto-Valdez, H.; Cerruti, P. From Nutraceutics to Materials: Effect of Resveratrol on the Stability of Polylactide. *ACS Sustainable Chem. Eng.* **2014**, *2*, 1534−1542.
(37) Iñiguez-Franco, F.; Soto-Valdez, H.; Peralta, E.; Ayala-Zavala, J. F.; Auras, R.; Gámez-Meza, N. Antioxidant Activity and Diffusion of Catechin and Epicatechin from Antioxidant Active Films Made of Poly(l-lactic acid). *J. Agric. Food Chem.* **2012**, *60*, 6515−6523.
(38) Zuidam, N. J.; Nedovic, V. A. *Encapsulation Technologies for Active Food Ingredients and Food Processing*; Springer: New York, 2010.

DOI: 10.1021/acssuschemeng.5b00446
ACS Sustainable Chem. Eng. 2015, 3, 2178−2186